

## Article

# Biological Characterization and Instrumental Analytical Comparison of Two Biorefining Pretreatments for Water Hyacinth (*Eichhornia crassipes*) Biomass Hydrolysis

Jitendra Kumar Singh <sup>1,†</sup>, Bhawana Chaurasia <sup>2,†</sup>, Anamika Dubey <sup>1,†</sup>, Alexis Manuel Faneite Noguera <sup>3,†</sup> , Aditi Gupta <sup>4</sup>, Richa Kothari <sup>5</sup>, Chandrama Prakash Upadhyaya <sup>2</sup>, Ashwani Kumar <sup>1,\*</sup>, Abeer Hashem <sup>6,7</sup>, Abdulaziz A. Alqarawi <sup>8</sup> and Elsayed Fathi Abd Allah <sup>8</sup> 

- <sup>1</sup> Metagenomics and Secretomics Research Laboratory, Department of Botany, Dr. Harisingh Gour University (A Central University), Sagar 470003, M.P., India; rjpsingh12345@gmail.com (J.K.S.); anamikadubey909@gmail.com (A.D.)
  - <sup>2</sup> Department of Biotechnology, Dr. Harisingh Gour University (A Central University), Sagar 470003, M.P., India; chaurasia.bhawana02@gmail.com (B.C.); cpupadhyay@gmail.com (C.P.U.)
  - <sup>3</sup> Laboratory of Chemical Engineering, Faculty of Engineering, School of Chemical Engineering, University of Zulia, Guajira Avenue, Campus "Dr. Antonio Borjas Romero", Maracaibo 4001, Venezuela; afaneite@fing.luz.edu.ve
  - <sup>4</sup> Department of Chemistry, Sri Venkateswara College, Delhi University, Delhi 110021, India; 29.aditi@gmail.com
  - <sup>5</sup> Department of Environmental Science, Central University of Jammu, Samba 181143, India; kothariricha21@gmail.com
  - <sup>6</sup> Botany and Microbiology Department, College of Science, King Saud University, P.O. Box 2460, Riyadh 11451, Saudi Arabia; habeer@ksu.edu.sa
  - <sup>7</sup> Mycology and Plant Disease Survey Department, Plant Pathology Research Institute, ARC, Giza 12511, Egypt
  - <sup>8</sup> Plant Production Department, College of Food and Agricultural Sciences, King Saud University, P.O. Box 2460, Riyadh 11451, Saudi Arabia; alqarawi@ksu.edu.sa (A.A.A.); eabdallah@ksu.edu.sa (E.F.A.A.)
- \* Correspondence: ashwaniitd@hotmail.com  
† Authors contributed equally.



**Citation:** Singh, J.K.; Chaurasia, B.; Dubey, A.; Faneite N., A.M.; Gupta, A.; Kothari, R.; Upadhyaya, C.P.; Kumar, A.; Hashem, A.; Alqarawi, A.A.; et al. Biological Characterization and Instrumental Analytical Comparison of Two Biorefining Pretreatments for Water Hyacinth (*Eichhornia crassipes*) Biomass Hydrolysis. *Sustainability* **2021**, *13*, 245. <https://doi.org/10.3390/su13010245>

Received: 27 November 2020

Accepted: 25 December 2020

Published: 29 December 2020

**Publisher's Note:** MDPI stays neutral with regard to jurisdictional claims in published maps and institutional affiliations.



**Copyright:** © 2020 by the authors. Licensee MDPI, Basel, Switzerland. This article is an open access article distributed under the terms and conditions of the Creative Commons Attribution (CC BY) license (<https://creativecommons.org/licenses/by/4.0/>).

**Abstract:** Water hyacinth is a rapidly growing troublesome aquatic weed plant, which causes eutrophication in water bodies and irreversible damage to the ecological system. In this work, we have investigated the water hyacinth biomass (WHB) hydrolysis efficacy of dilute alkaline (DA) pretreatment followed by biological pretreatment with white-rot fungus *Alternaria alternata* strain AKJK-2. The effectiveness of the dilute alkaline (DA) and biological pretreatment process on WHB was confirmed by using X-ray Diffraction (XRD) and Fourier Transform Infrared Spectrophotometer (FTIR), and was further visualized by Scanning Electron Microscope (SEM) and Confocal Laser Scanning Microscopy (CLSM). XRD spectra showed the increase in the crystallinity of pretreated samples, attributed to the elimination of amorphous components as lignin and hemicellulose. FTIR peak analysis of pre-treated WHB showed substantial changes in the absorption of cellulose functional groups and the elimination of lignin signals. Scanning electron microscopy (SEM) images showed firm, compact, highly ordered, and rigid fibril structures without degradation in the untreated WHB sample, while the pretreated samples exhibited loose, dispersed, and distorted structures. XRD indices (Segal, Landis, and Faneite), and FTIR indices [Hydrogen bond intensity (HBI); Total crystallinity index (TCI); and Lateral order crystallinity (LOI)] results were similar to the aforementioned results, and also showed an increase in the crystallinity both in alkaline and biological pretreatments. Alkaline pretreated WHB, with these indices, also showed the highest crystallinity and a crystalline allomorphs mixture of cellulose I (native) and cellulose II. These results were further validated by the CLSM, wherein fluorescent signals were lost after the pretreatment of WHB over control. Overall, these findings showed the significant potential of integrated assessment tools with chemical and biological pretreatment for large-scale utilization and bioconversion of this potential aquatic weed for bioenergy production.

**Keywords:** water hyacinth biomass (WHB); sustainability; sodium hydroxide pretreatment (NaOH); biological pretreatment; crystallinity index; bioethanol

## 1. Introduction

Bioethanol is used as a sustainable eco-friendly alternative to conventional fossil fuels for mitigating the global energy problem, and a reduction in greenhouse gases [1–3]. The conflict between food and fuel for the production of first-generation bioethanol from starch and sugary food resources is a major issue from the food safety point of view [4,5]. Therefore, to circumvent the competition with food, the utilization of profusely available and non-edible plant parts, including agricultural crop wastes and fast-growing aquatic weed plants as a feedstock, is being attempted nowadays [6–9]. Water hyacinth (*Eichhornia crassipes*; Family-Pontederiaceae, related to the Liliaceae family) is a competent cellulosic biomass for the generation of renewable fuels (second-generation ethanol) as well as a source of sustainable energy because it has a high carbohydrate and low lignin content compared to other biomass types, and because of its indiscriminate invasive production in some aquatic ecosystems [10,11]. Its usage could help to intervene with and ease the environmental problems caused by this highly invasive weed in water bodies [8,12]. In water hyacinth biomass (WHB), the amount of lignin (10%) is less, and the amount of cellulose (20%) and hemicelluloses (33%) are high [8]. This plant depletes oxygen, increases biological oxygen demand, and disturbs the nutrient balance between water bodies, which results in reducing aquatic biodiversity and increasing the rate of evapotranspiration, which could alter irrigation, shipping, and fishing [8]. It is extremely difficult to eradicate this invasive weed by using biological, chemical, and physical methods, therefore a method is urgently needed for its rapid disposal along with its biotechnological benefits [8,13]. Many recent studies have showed its potential for the production of biogas [14,15], charcoal briquettes blended with molasses, which could be used as fuel in rural areas [16], biodiesel [17], and carboxymethyl cellulose [18].

Enzymatic hydrolysis of lignocellulosic biomass is the most promising and effective approach for getting a higher glucose yield [19]. Different pretreatment methods are used to achieve efficient enzymatic hydrolysis of biomass, which provides an effective surface area for enzymes to hydrolyze the cellulose and hemicelluloses by reducing cellulose crystallinity, removing the lignin moieties, and thereby increasing the fraction of amorphous cellulose. The correct understanding about the inter and intramolecular changes that occur to lignocellulosic materials during the fundamental processes of biorefining as conditioning and pretreatment, is the basis for the future models to design biorefineries [5,20].

The cell wall of the plant is exposed to complex, heterogeneous interactions of lignin, hemicellulose, and cellulose, which prevent the cell wall from being inaccessible to microorganisms and enzymes during their facile bioconversion to sugars and other intermediates at high yields [21]. The removal of some recalcitrant compounds, including various forms of uronic acid, acetyl groups, and lignin from lignocellulosic biomasses, is an essential duty of a pretreatment technique. In the last 5 years, researchers have studied several pretreatment methods for ethanol production from water hyacinth, like peroxide, pretreatment using  $H_2O_2$  [22], peroxide/alkaline pretreatment using  $H_2O_2$  and NaOH, respectively [23], alkaline pretreatment using NaOH [22,24,25], acid pretreatment using  $HNO_3$  and HCl [24], Imidazolium based ionic liquids [8] and  $H_2SO_4$  [22,24,26], and biological pretreatment using bacteria [27] and white-rot fungi (*Penicillium chrysosporium*) [28].

Although there are several pre-treatment methods available, among them, biological pretreatment seems to be the most promising as a green eco-friendly process because there is no inhibitor generated during the process. At present, there are few limitations in utilizing this approach for a pilot-scale study like a long incubation time for effective delignification, which can be reduced to some extent by using a suitable consortium of microbes. There is an urgent need for research and development activities and fine-tuning of the process for the improvement of an economically feasible method.

Therefore, the primary aim of this study was to compare the effect of two pretreatment techniques, like dilute alkaline (DA) pretreatment with NaOH and biological pretreatment,

with the lignocellulosic degrading fungus *Alternaria alternata* on water hyacinth biomass (WHB). We analyzed post pretreatment biomass using non-destructive, Fourier Transform Infrared Spectrometer, Scanning Electron Microscopy, X-ray Diffraction, and Confocal Laser Scanning Microscopy, to see the changes in the WHB. We show the whole experimental workflow used in this study (Figure 1).

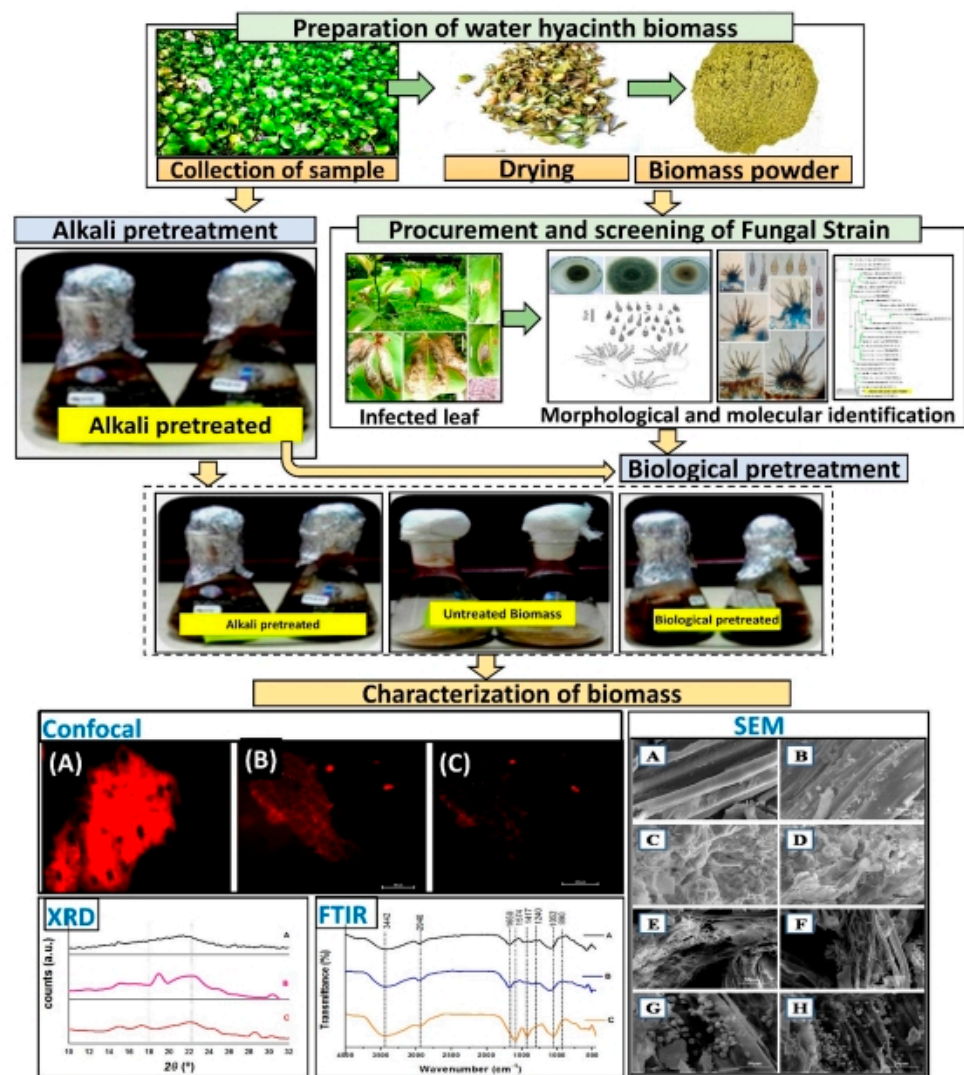


Figure 1. Experimental workflow.

## 2. Materials and Methods

### 2.1. Sample Preparation

Water hyacinth biomass (WHB) was collected locally from the Lakha Banjara Lake, ( $23^{\circ}50''$  North:  $78^{\circ}45''$  East) near Sanjay drive, Sagar, (M.P), India. The stem and leaves of WHB were washed with tap water after the removal of roots, and were cut into pieces and dried in an oven at  $60^{\circ}\text{C}$  [8]. The dried WHB sample was grounded and kept in a labeled plastic bag at  $4^{\circ}\text{C}$  to prevent any possible degradation for further use [8].

### 2.2. Procurement and Screening of Fungal Strain

Several fungal samples were collected from the infected trees near the University Campus (Dr. Harisingh Gour University, Sagar, India), but based on their cultivability in the lab and lignocellulose degrading ability, only *Alternaria alternata* was cultured on Potato Dextrose Agar medium (PDA) and incubated at  $37^{\circ}\text{C}$  for about 5 days. This fungal strain was identified morphologically, microscopically, and molecularly (18S rRNA). This fungal

strain was screened for its cellulase producing ability by following the methods [29] with slight modification.

### 2.3. DNA Extraction and Molecular Identification of the Fungal Isolate

Genomic DNA of the fungal strain was isolated by using an Insta Gene Matrix Genomic DNA isolation kit and PCR amplified by using ITS1 forward primer (5'-TCCGTAGGTGAACCTGCGG-3') and ITS54 reverse primer (5'-TCCTCCGCTTATTGATATGC-3'). ABI 3730x1 sequencer (Applied Biosystems) was used for sequencing amplified fungal DNA. The obtained sequence was compared with other similar sequences available in the GenBank database through the NCBI BLAST software available at <http://www.ncbi.nlm.nih.gov/blast/Blast.cgi>. The phylogenetic tree for the fungal strain was constructed by using iTOLv4 (interactive tree of life) after building a similar relationship between the similar sequences [30].

### 2.4. Pretreatment and Fermentation Methods

#### 2.4.1. Dilute Alkaline (DA) Pretreatment of Water Hyacinth Biomass (WHB)

Dilute alkali (DA) pretreatment was performed by soaking 100 g of WHB (5 wt%) in 2% NaOH (HiMedia, Mumbai, India) solution for about 10 min at room temperature. Then, this mixture was kept in a water bath at 100 °C for 2 h with manual mixing after every 10 min. After pretreatment with DA, WHB was washed several times with hot distilled water for complete removal of alkali residue until the pH of the filtrate reached 7. These DA pretreated WHB samples were then dried overnight at 60 °C and kept at 4 °C for further analysis.

#### 2.4.2. Biological Pretreatment of WHB

The process of biological pretreatment by using fungal strain was performed in 250 mL Erlenmeyer flasks using solid-state fermentation (SSF) [31,32]. For this, 5 g of WHB (0.2 mm size) were appended with 10 mL of minimal salt media (MSM) to obtain the appropriate substrate moisture content and suspended in 250 mL flask and inoculated by *Alternaria alternata*. Erlenmeyer flasks were maintained statically at 37 °C up to 15 days in triplicates [28]. The samples were collected after a 1, 3, 6, 9, 12, and 15 day's incubation period. A set of non-pretreated WH biomass served as a control. The biologically pretreated WHB was collected in the buffer by centrifugation for 10 min at 5000 rpm. The substrate was then washed with distilled water, dried in an oven at 60 °C, and stored in moisture-free plastic bottles at 4 °C for further analysis.

### 2.5. Characterization of Pretreated WHB

Non-destructive methods were used to analyze the changes that took place before and after dilute alkali (DA) and biological pretreatment in WHB.

#### 2.5.1. X-ray Diffraction (XRD) Analysis

Pretreated and untreated samples of WHB were analyzed by X-ray diffraction (AXS-D8 Advance Bruker diffractometer, Karlsruhe, Germany), using  $\text{Cu}_{K\alpha}$  ( $\lambda = 1.54 \text{ \AA}$ ) radiation at 30 kV and 30 mA, with a grade range between 10° and 60°, a speed of 2° min<sup>-1</sup>, and a step size of 0.05° at room temperature; samples were held on a quartz sample holder [8]. Spectra obtained were smoothed and normalized. Spectra were visually inspected for crystalline cellulose allomorphs patterns caused by the different processes of conditioning (drying) and pretreatment applied to the WHB, in the case of the aqueous alkaline pretreatment [33]. The crystallinity index along with the intensity of the main crystalline plane (002) and the amorphous fraction was calculated using the intensity between 18° and 19° for cellulose I and between 13° and 15° for cellulose II, for the amorphous fraction ( $I_{am}$ ), and the maximum intensity between 22° and 23° for cellulose I and between 18° and 22° for cellulose II, for the crystalline fraction ( $I_{002}$ ) [34].



Biomass crystallinity is an important characteristic feature affecting the enzymatic hydrolysis. A new expression proposed for the crystallinity index of lignocellulosic biomass (only for Cellulose I), based on the Segal [35] and Landis [36] equations (Equations (1) and (2), respectively), and which takes the crystallinity of microcrystalline cellulose as a reference, was used to see the effect of pretreatments on the elimination of components of an amorphous crystalline structure in the WHB. The Faneite percent crystallinity index ( $\%CrI_{Faneite}$ ) was calculated by the following Equation (3) [33].

$$\%CrI_{Segal} = \left(1 - \frac{I_{am}}{I_{002}}\right) \cdot 100\% \quad (1)$$

$$CrI_{Landis} = \frac{2 \cdot I_{002}}{I_{am}} \quad (2)$$

$$\%CrI_{Faneite} = 14.5547 \cdot \frac{I_{002}}{I_{am}} \% \quad (3)$$

$$\%CrI_{segal} = \left(1 - \frac{I_{am}}{I_{002}}\right) \times 100\%$$

As a point of reference for comparison, for the changes in crystallinity due to the alkaline pretreatment, concerning the literature, the expression of extended severity parameter ( $R'$ ) of Chum et al., [37] (Equation (4)) was used.

$$R' = [X] \cdot e^{\frac{T-100}{14.75} \cdot t} \quad (4)$$

where  $[X]$ , is the acidity or alkalinity, if the pretreatment is with acid or with alkali, expressed in concentration ( $\text{mol L}^{-1}$ ) of  $\text{H}^+$  ion or  $\text{OH}^-$  ion, respectively;  $T$  is temperature in  $^{\circ}\text{C}$  and  $t$  is time in min.

## 2.5.2. Fourier Transform Infrared Spectrometer (FTIR)

FTIR spectroscopy was conducted by using a Fourier Transform Infrared Spectrophotometer (8400S SHIMADZU, Kyoto Japan). FTIR analysis was used to monitor the changes in the structural and functional group when pretreated with alkali and with biological pretreatment. A total of 10 mg of dried WH biomass was mixed with 200 mg of spectroscopic grade KBr (Merck, India) and was grounded into a fine powder and then pressed into pellets for IR transmission studies. Pure KBr was recorded in each run [8,38]. The FTIR spectra were generated with an average scan of 64 scans in the range of  $400 \text{ cm}^{-1}$ – $4000 \text{ cm}^{-1}$  with a resolution of  $2 \text{ cm}^{-1}$ . Spectra in terms of wavenumber ( $\text{cm}^{-1}$ ) versus transmittance were smoothed and normalized.

The most important FTIR indices to see changes in the crystalline characteristics of the WH cellulose were calculated. Hydrogen bond intensity ( $HBI$ ) is the absorbance ratio between the elongation of O-H groups, and the skeletal vibration of the groups C-C and C-O (Equation (5)). The total crystallinity index ( $TCI$ ) is the absorbance ratio between the flexion of O-H groups and the elongation of C-H groups (Equation (6)). Lateral order crystallinity ( $LOI$ ) is the absorbance ratio between the flexion of C-H<sub>2</sub> groups and the  $\beta$ -glycosidic bonds (Equation (7)).

$$HBI = \frac{A_{3338\text{cm}^{-1}}}{A_{1334\text{cm}^{-1}}} \quad (5)$$

$$TCI = \frac{A_{1375\text{cm}^{-1}}}{A_{2900\text{cm}^{-1}}} \quad (6)$$

$$LOI = \frac{A_{1420\text{cm}^{-1}}}{A_{893\text{cm}^{-1}}} \quad (7)$$

The absorption band between 1420 and 1430  $\text{cm}^{-1}$  is associated with the amount of the crystalline structure of the cellulose, while the band at 897  $\text{cm}^{-1}$  is assigned to the amorphous region in cellulose [34,39]. The ratio between these two absorption bands was defined as an empirical crystallinity index proposed firstly by Nelson and O'Connor [34] or as a Lateral Order Index (*LOI*) proposed by Hurtubise and Krassig [40]. Subsequently, Nelson and O'Connor [34] defined the Total Crystalline Index (*TCI*) as the absorbance ratio of 1372  $\text{cm}^{-1}$  and 2900  $\text{cm}^{-1}$  bands. In addition, Nada et al. [41] introduced Hydrogen Bond Intensity (*HBI*), which is related to the crystal system and the degree of intermolecular regularity as well as the amount of bound water. *HBI* was used to study the changes of hydrogen bonding between certain hydroxyl groups in cellulose; generally, crystallinity decreases with an increasing *HBI* value [42]. This parameter was determined by the absorbance ratio from 3350  $\text{cm}^{-1}$  and 1318  $\text{cm}^{-1}$  bands. *TCI* is proportional to the crystallinity degree of cellulose, while *LOI* is correlated to the overall degree of order in cellulose [43].

#### 2.5.3. Scanning Electron Microscopy (SEM) Analysis

For Scanning Electron microscopy (SEM), an untreated and pre-treated dried solid WH biomass sample was coated with a gold sputter and observed under FEI NOVA NANO SEM 450 and SN 9921187 (United State) operated with an acceleration voltage of 15 kV and a working distance of 5 mm [8]. SEM images at different magnifications were recorded.

#### 2.5.4. Confocal Laser Scanning Microscope (CLSM) Analysis

The fluorescent microscopic images of pre-treated and untreated WHB were recorded using a Confocal Laser Scanning Microscope (MEA53100, Nikon Corporation, Japan) with two laser sources (465–495 nm and 615 nm). The CLSM was used to capture fluorescent images of DA pre-treated and untreated WHB, then these images were used for analyzing the degradation of WHB by stain binding assay. The sample images were directly taken at 40X and 10X objectives with instruments auto-exposure function and by using NIS-Elements AR 4.20.00 (Build 967) 64 bits software. The fluorescence of particles was visualized at an excitation range of 465–495 nm and emission result of 615 nm. The photomicrographs at a single focus were imaged under differential interference contrast (DIC) as a fluorescent image. Microstructure determination based on the distribution of lignin with auto-fluorescence and samples were stained with 0.1% safranin for 5 min. The stained WHB samples were further dehydrated with a serial dilution of ethyl alcohol (50%, 70%, 90%, and 100%) followed by mounting in 70% glycerol [44] and were allowed to dry in the dark. Samples were observed at different resolutions of 100  $\mu\text{m}$ , 50  $\mu\text{m}$ , and 10  $\mu\text{m}$  under CLSM.

#### 2.6. Graph Preparation

Origin trial version 2020 (Origin Corporation, Northampton, MA, USA) software was used for data analysis and Graph preparation.

### 3. Results and Discussion

#### 3.1. Morphological Identification of Fungal Isolates AKJK2

For this experiment, the fungus was obtained from the upper surface of leaves of *Smilax purhampuy* Ruiz at the site of Suatala; district Sagar, Madhya Pradesh, India. The fungal strain isolated from the forest showed a variety of morphological characteristics. The amphigenous lesion is initially small on a leaf; at maturity, these lesions spread on the whole leaf with regular effuse colonies that are amphiphylous, black, include the mycelium of hyphae and well-developed stroma, and conidiophores, which arise in a group that is straight, flexuous, simple, or branched. Sometimes, these colonies are accompanied by brownish or smooth conidiophores that are solitary, obclavate ellipsoidal, have a small to large beak, and have 1–8 transverse and oblique features that are often constricted at the septa. This fungus isolate, when grown aseptically on CMC agar plates, has shown a positive result for cellulase production activity.

### 3.2. Molecular Identification of Fungus Strain

Based on a NCBI blast of obtained fungal sequence, this strain was found to be closely linked to *Alternaria alternata* (gene bank accession no. GenBank MW300285). An interactive tree of life tool (iTOL) was used to construct a phylogenetic tree by establishing a relationship of this fungal strain with another closely related genera (Figure 2).

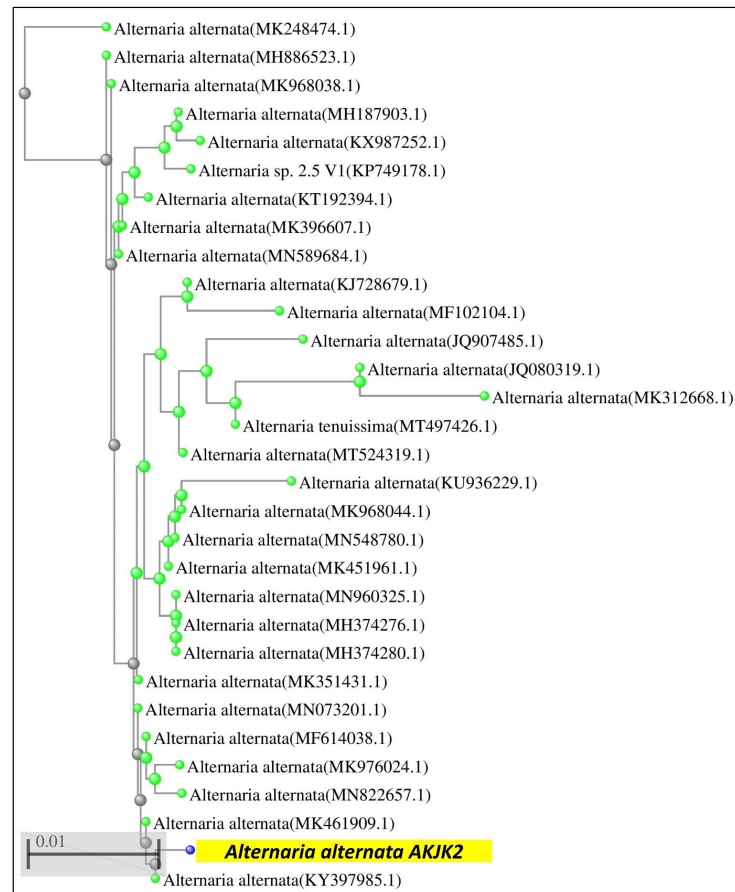


**Figure 2.** Phylogenetic tree showing the evolutionary relationship between fungal isolate and other reference strains from the GenBank database.

### 3.3. X-ray Diffraction (XRD)

The smoothed and normalized diffractograms of XRD analysis of untreated WHB (A), pretreated WHB with alkaline pretreatment (B), and with biological pretreatment (C), within the range of  $2\theta$  where the signals of interest can be seen are presented in Figure 3. In general terms, the treated biomass generates better-defined signals than the untreated one, which shows the elimination of non-crystalline components due to the effects of pretreatments, added to a slight increase in the signals that denote the crystalline structure of cellulose [33,45,46]. The spectrum generated by the untreated WHB is typical for this biomass [45] and for the biomass of other aquatic plants such as lemna [33], where a substantial increase in the baseline is appreciated in the value of  $2\theta$  where the peak of the 002 planes should be, without defining the rest of the planes. Manivannan and Narendhirakannan [45], obtained slightly more defined peaks in their samples of untreated WHB, which can be attributed to the fact that they have used the most fibrous components of this plant or that they have used non-young plants as samples.

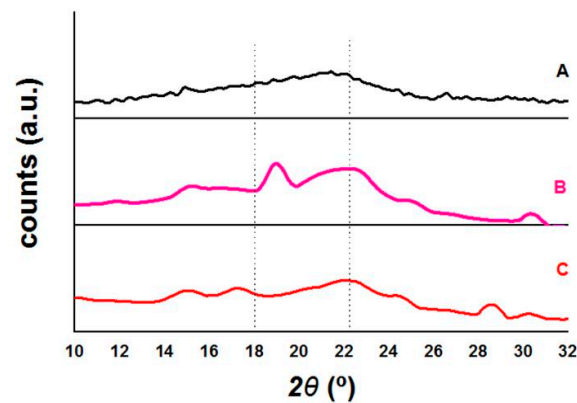


**Figure 3.** X-ray Diffraction (XRD) patterns of untreated and pretreated water hyacinth (WH) biomass samples: (A) Untreated (WHB); (B) Dilute alkaline (DA) pretreated; (C) Biological pretreated.

The pattern for WHB pretreated with biological pretreatment indicates that of cellulose I, with its two signals at approximately  $15^\circ$  and  $17^\circ$  of the  $2\theta$  axis and the main signal, more intense, at  $22^\circ$ , of the  $2\theta$  axis. WHB treated with alkaline pretreatment, on the other hand, presents a pattern that looks like a mixture of cellulose I and II, due to the two peaks between  $18^\circ$  and  $22^\circ$  of the  $2\theta$  axis, and a poor signal at  $12^\circ$  of the  $2\theta$  axis. The process of drying a very wet material, grinding, re-wetting in pretreatment, and then re-drying can lead to the rearrangement of cellulose crystals towards their most thermodynamically stable allomorph, which is cellulose II [47]. Similar results were obtained by Pothiraj et al. [45] for their WHB treated with alkaline pretreatment because of their diffractograms, without them having reported this, but not for Manivannan and Narendhirakannan, [46], who used an acid pretreatment. This is because the acid produces the degradation of the cellulose chain, but the alkali does not but does interact with the cellulose, generating an inter-crystalline swelling, then, when washing and drying, the cellulose recrystallizes [48]. This process is called mercerization, and although concentrated alkali is used in mercerization, there is no doubt that this effect to a lesser extent occurs in diluted alkaline pretreatments. In Table 1, the crystallinity indices for the samples of this work and the WHB samples of Pothiraj et al. [45] and Manivannan and Narendhirakannan [46] are presented, calculated from their spectra. There is no doubt that the pretreatments applied to WHB, whether biological or chemical, remove amorphous material, leaving crystalline cellulose exposed for subsequent biorefining processes. Of the 3 indices studied, the Faneite index has more coherent numerical values concerning what is seen in the spectra (with respect to Segal), and is also easier to interpret than the Landis index. For example, the increase in the Segal crystallinity of the untreated WHB compared to the biologically pretreated one is 32.84%, while the increase is 4.73% when using the Faneite crystallinity, which is consistent with the slight increase seen in the spectra (Landis reports the same changes as Faneite). This is because the Faneite index uses the crystallinity of the microcrystalline cellulose as a proportionality factor, which circumscribes it to the specific area of the biomass, and also places all the spectra in relation to it [33], thereby allowing a more normalized comparison. The only limitation is that it is used only for Cellulose I.



**Table 1.** Crystallinity index of the untreated, dilute alkaline (DA) pretreated, and biological pretreated WHB determined using XRD.

S. No.	Specimen	Crystallinity Indices		
		Segal (%)	Landis	Faneite (%)
1	Untreated	12.09	2.28	16.56
	NaOH pretreatment ( $R' = 61.23$ )	20.05	2.50	18.21
2	(as Cellulose I)	35.79	3.11	—
	(as Cellulose II)	16.06	2.38	17.34
3	Biological pretreatment			
<b>Pothiraj et al. [45]</b>				
	Untreated <sup>1</sup>	33.33	3.00	21.83
	Ca(OH) <sub>2</sub> pretreatment ( $R' = 24.29$ )	37.06	3.18	23.13
	(as Cellulose I) <sup>1</sup>	42.64	3.49	—
	(as Cellulose II) <sup>1</sup>			
<b>Manivannan &amp; Narendhirakannan [46]</b>				
	Untreated <sup>1</sup>	41.96	3.45	25.08
	H <sub>2</sub> SO <sub>4</sub> pretreatment ( $R' = 51.05$ ) <sup>1</sup>	42.69	3.49	25.40

<sup>1</sup> Values calculated from the reported spectra.

Of the two pretreatments studied, the diluted alkaline allowed a greater removal of amorphous components, since the biological treatment only increased Faneite crystallinity by 4.73%, which is half the increase registered for the alkaline pretreatment. The increase in the crystallinity in biological pretreatment is attributed to the removal of lignin and hemicellulose in the amorphous region [49]. However, this process is also accompanied by an elimination of glycosidic bonds from cellulose which also generates a decrease in crystallinity [50], which is in agreement with the lower increase in the crystallinity of the biological pretreatment compared to the alkaline one.

The crystallinity indices of the untreated WHB samples, and likewise, their cellulose content, are closely related, and depend on many factors, such as the age of the samples, the components of the plant used for said samples, among others. The cellulose content reported by Pothiraj et al. [45] for their untreated WHB samples, was 20.2%, while for Manivannan and Narendhirakannan [46], it was 35.84%, with their Faneite crystallinity being 21.83% and 25.08%, respectively, which corroborates the aforementioned results. The samples of this work must have a lower amount of cellulose than the samples of the aforementioned works, which is not necessarily a disadvantage since it can be a sign of a higher concentration of proteins or hemicellulose, which is equally useful for the production of bioethanol. The Faneite crystallinity of untreated WHB, concerning other lignocellulosic materials, is within the range of grasses, where the leaves and bagasse of sugarcane are also found [33].

In relation to the increase in crystallinity, with the increase in severity of the pretreatments, the results of this work and those of the literature (for chemically similar pretreatments), as a whole, are quite coherent. For a severity of 61.23, the increase in Faneite crystallinity was 9.96% for the WHB of this work, while a severity of 24.29 generated an increase in Faneite crystallinity of 5.93% for the samples of Pothiraj et al. [45]. Although the pretreatment of Manivannan and Narendhirakannan [46] was carried out with an intermediate severity of 51.05, the increase in crystallinity did not result in an intermediate numerical value, since it was only 1.27%, and this was attributed to the fact that these are reactions of a different nature and which generate different changes in the paracrystalline structure of cellulose. The Segal and Landis crystallinities calculated with the intensities of cellulose I and II for the samples treated with alkaline pretreatment, which were used for this work and that of Pothiraj et al. [45], show a predominance in cellulose II, which is attributed to the fact that although low alkali concentrations were used, the reaction times (120 min to 180 min, respectively) and temperature (100 °C) were high,

which was considered to have contributed to the mercerization of an important fraction of the native crystalline cellulose.

### 3.4. Fourier Transform Infrared Spectrometer (FTIR)

FTIR spectra of untreated biomass (A), dilute alkaline (B), and biological pretreatment of WHB (C) are presented in Figure 4. FTIR analysis presents relative values from amorphous and crystalline areas and is a suitable tool for the examination of crystallinity changes during the pretreatment [51]. The FTIR spectral data indicate the existence of lignin, cellulose, and hemicellulose, which are the main components of WHB [8]. The peak ranges from  $800\text{ cm}^{-1}$  and  $4000\text{ cm}^{-1}$  of different band spectrums comprise the presence of major components of lignin, cellulose, and hemicelluloses. The intense broadband between  $3000\text{ cm}^{-1}$  and  $3750\text{ cm}^{-1}$  is attributed to the stretching vibrations of  $-\text{OH}$  [52], and it is absorbed more in the material treated with alkaline pretreatment, and even more in the biological pretreatment, which is not in agreement with the increase in crystallinity; this may be due to the mixture of cellulose I and II in the material pretreated with alkali.

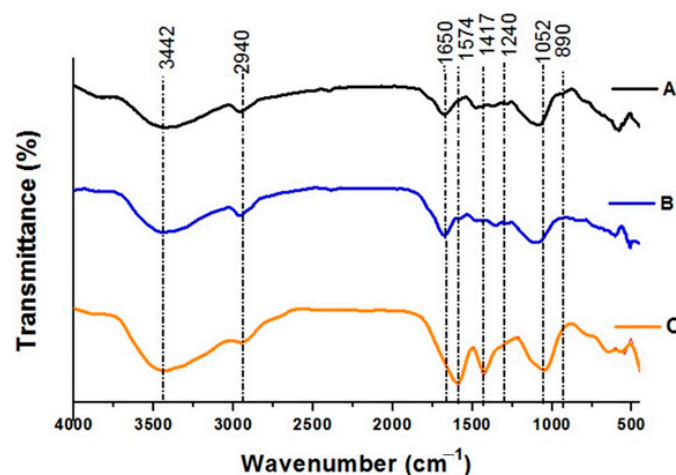


**Figure 4.** FTIR spectra of untreated and pretreated water hyacinth (WH) biomass: (A) Untreated WHB, (B) Dilute alkaline (DA) pretreated WHB, (C) Biological pretreated WHB.

This increase is the expected response of a material to which access barriers to cellulose were eliminated; the band between  $2800\text{ cm}^{-1}$  and  $3000\text{ cm}^{-1}$ , approximately, and the small band around  $2373\text{ cm}^{-1}$  are attributed to the stretching vibrations of  $-\text{OH}$ , and C-H in the  $\text{CH}_2$  and  $\text{CH}_3$  groups [52] which are slightly more absorbed in the alkaline pretreatments such as that obtained by Pothiraj et al. [45] and they are blurred in the biologically treated material, which is in agreement with what was found by Manivannan and Narendhirakannan [46].

The band around  $1790\text{ cm}^{-1}$  and  $1500\text{ cm}^{-1}$  is attributed to the adsorbed water [43] with a maximum at  $1650\text{ cm}^{-1}$  for the untreated WH and the alkali pretreated WH, and displaced towards  $1574\text{ cm}^{-1}$  for the pretreated material with biological pretreatment; these results led to an increase in crystallinity, which results from the greater exposure of cellulose that was obtained through pretreatments. This increase, which was greater for the biological treatment, can be explained by the intense mixing with an aqueous solution in the alkaline treatment, and by the longer exposure time of the material in the process of the elimination of access barriers to cellulose, during the biological treatment. The increase in crystallinity is not associated with the hygroscopicity of cellulose concerning the outer protective layers of the plant tissue, which are areas that are rich in lignin [49]. The band at  $1417\text{ cm}^{-1}$ , corresponding to  $\text{CH}_2$  scissoring at C(6) in cellulose [43], which is considerably defined in the biological treatment, demonstrates the increase in crystallinity in the material subjected to this pretreatment. Although the WH alkaline pretreated was more crystalline

than the native biomass, the presence of cellulose II causes the blurring of this band [34], which agrees with what was seen in the XRD result.

The reduction of the two very small bands, between  $1325\text{ cm}^{-1}$  (not shown in Figure 4) and  $1240\text{ cm}^{-1}$ , attributed to C-H deformation in hemicelluloses, and C-O stretching in lignin and hemicellulose, respectively, is the indication of the removal of fractions of lignin and hemicellulose, due to the pretreatments, which is in agreement with the results of Manivannan and Narendhirakannan [46]. On the other hand, the increment of the band around  $1050\text{ cm}^{-1}$  (C-O stretching vibration of the cellulose structure) showed the highest proportion of cellulose in the pretreated WH, which is in agreement with Pothiraj et al. [45]. The mixture of allomorphs (Cellulose I and II) in the sample pretreated with alkali may have influenced that fact that this band does not absorb more, as observed in the valley of  $3442\text{ cm}^{-1}$  of the same spectrum. The small band of around  $890\text{ cm}^{-1}$ , corresponding to glycosidic bonds [45], blurs with pretreatments, which is related to the increase in crystalline regions in the material, as observed by Nelson and O'Connor [34] in their work. Table 2, summarizes the TCI, LOI, and HBI values for untreated, DA, and biological pretreated WHB.

**Table 2.** HBI, TCI, and LOI index of untreated, NaOH, and biological pretreated water hyacinth (WHB) biomass samples.

S. No.	Specimen	FTIR Indices		
		HBI 3338/1334 ( $\text{cm}\cdot\text{cm}^{-1}$ )	TCI 1370/2925 ( $\text{cm}\cdot\text{cm}^{-1}$ )	LOI 1420/897 ( $\text{cm}\cdot\text{cm}^{-1}$ )
1	Untreated	2.0849	0.7662	2.9920
2	NaOH pretreatment	1.1833	1.3409	1.0702
3	Biological pretreatment	1.6490	1.1245	3.8592

LOI, lateral order index or crystallinity index; TCI, total crystallinity index; HBI, hydrogen bond intensity.

All of the results of FTIR indices occurred following XRD results. The HBI, on the one hand, decreased for the sample that was treated biologically, but even more for the one treated with alkali, which is in accordance with the behavior expected for this index in terms of the order in crystallinity [42]; this result is a contrast to the TCI, which increased for the biological sample, and even more so for the alkali-treated sample [34]. Regarding the LOI, although it increased for the sample that was treated biologically, it decreased to almost 1 in the sample treated with alkali, which was the expected result, according to the deduction reached when analyzing the [34] spectra, and which is attributed to the mixture of crystalline allomorphs of cellulose I and II, presented in this sample.

### 3.5. Scanning Electron Microscopy (SEM)

The structural changes of dilute alkaline pretreated, biologically pretreated, and biologically untreated WHB visualized by using SEM are presented in Figure 5. The untreated WHB sample showed a rigid and smooth surface, since fibrillates were all intact (Figure 5A,B). However, after DA pretreatment, samples showed cellular deformation and loosening of fibers (Figure 5C,D). As shown in the images, the raw fibrous structure has been completely disorganized; the surface has become loose and swollen after pretreatment with DA. Also, Carvalho et al. [31] reported that alkaline pretreatment causes fiber swelling and, in turn, results in separation of the fiber linkages between carbohydrates and lignin. However, more prominent structural changes were observed in the biological pretreatment than in the DA pretreated sample (Figure 5E,F).

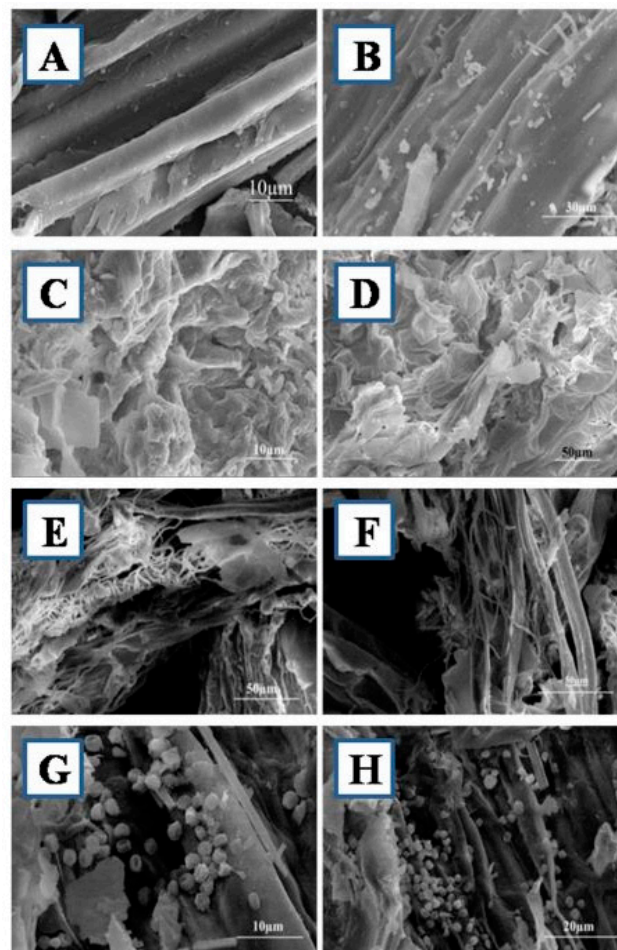


**Figure 5.** SEM images of water hyacinth biomass; (A,B)—untreated biomass (X1500); (C,D)—Dilute alkaline (DA) pretreated WHB (X1500); (E–H)—Biological pretreated WHB (X1500).

Pretreatment of WHB with the fungus *Alternaria alternata* resulted in extensive damage, giving more disorganized fibers with large pore size. This greater porosity likely indicates that xylanases can degrade the xylan matrix that holds cellulose microfibrils [53]. This disruption of the fibers confirms that the microbial attack causes alteration of the fibrils at a molecular level. The surface area of the biological pretreated samples showed pores and cracks. The fragile surface area is attributed to the weakening of the cell wall during delignification that allows more efficient solubilization of cellulose, and therefore, a higher yield of reducing sugars. Moreover, the *Alternaria alternata* strain AKJK2 growth conditions might have had some effect on the structural modification, as alkaline conditions are known to promote solubilization of lignin [32]. The biological pretreatment of WHB samples undoubtedly portrayed increased surface roughness as compared to that of untreated and DA pretreated WHB, which indicates that a modified structure may allow cellulases access to the internal cellulose surface or enhanced exposure of cellulose microfibrils. Similar results were found in the study conducted by Taniguchi et al. [54], wherein they have used *Pleurotus ostreatus* and reported an increase in the susceptibility of rice straw to enzymatic hydrolysis due to the partial degradation of lignin. This structural alteration is similar to those observed in lignin removal by fungal pretreatment [28].

### 3.6. Confocal Laser Scanning Microscopy (CLSM)

Confocal microscopy was used to investigate the surface morphologies of (A) untreated WHB, (B) Dilute alkaline (DA) pretreated WHB, and (C) Biological pretreated (WHB) at microscales. Clear differences were observed by confocal fluorescence imaging

in the extent of physical alteration of the WHB upon pretreatments (Figure 6A,B). CLSM images showed the lignin distribution in WHB with fluorescing, at 568 nm which is specific to lignin. From (Figure 6A) it was observed that the cell wall areas are more lignified in untreated WHB that showed a stronger fluorescence (as indicated in red).

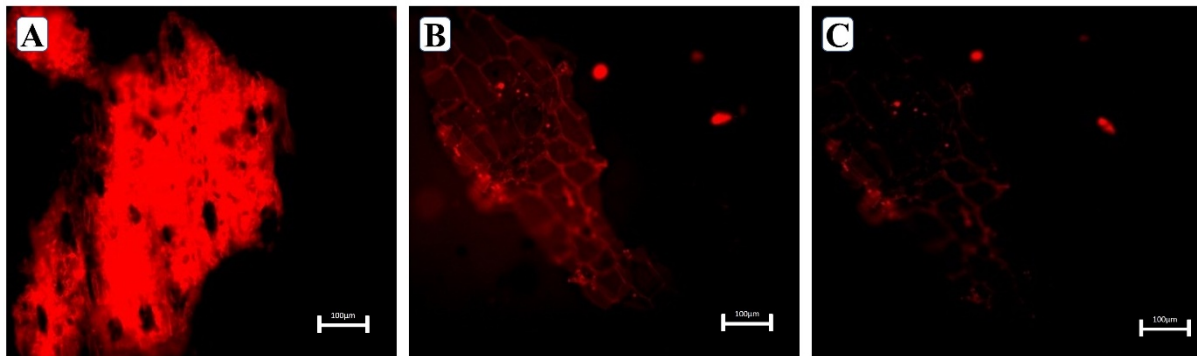


**Figure 6.** CLSM images of water hyacinth biomass (WHB): (A) untreated WHB; (B) Dilute alkaline (DA) pretreated WHB; (C) Biological pretreated (WHB).

However, the fluorescence intensity in the pre-treated WHB shown in Figure 6B indicates that the lignification level is lower as compared to the untreated WHB, which confirms the degradation of lignin by biological pretreatment. Singh et al. [55] showed that the Ionic Liquid pretreated corn stover samples do not show any resemblance to the untreated samples, and also do not fluoresce, indicating that no or very low lignin in the sample. The obtained result of this study is well corroborated with the work where the cell wall of switchgrass after biological pretreatment showed less fluorescence intensity due to lignin degradation [56]. The study conducted by Saha et al. [28] showed that the biological pretreatment of corn stover with white-rot fungus enhances enzymatic hydrolysis. Our study was corroborated with the study conducted by Dong et al. [57], which shows the efficient delignification significantly increased the digestibility and accessibility of cellulase to biomass, thereby improving the saccharification efficiency by using CLSM coupled with fluorescent labeling.

#### 4. Conclusions

In this work, characterization of (A) untreated WHB, (B) Dilute alkaline (DA) pretreated WHB, and (C) Biological pretreated (WHB) was done by using FTIR, XRD, SEM, and CLSM methods, which are a largely non-destructive and rapid way to analyze hydrolyzed substrates. X-ray diffraction patterns showed increases in WHB crystallinity with the dual application of alkaline and biological pretreatments. The Faneite index, which is used for effective FTIR analysis, resulted in more consistent and easy-to-understand numerical values, but only for samples without cellulose I. The FTIR analysis showed the elimination of non-polysaccharide components of the treated samples, both biologically and with alkaline, prevailing at the end, involving signals referring to the cellulose and hemicellulose chain. Through the indices of the FTIR analysis: HBI, TCI, and LOI, the increase in crystallinity caused by both pretreatments was confirmed, following the same order found through the XRD indices, as well as the mixture of cellulose I and II, which is generated in alkaline treatment. The SEM study shows the effectiveness of the pretreatment process for the clear observation of the elimination of the components that serve as a barrier towards cellulose, on the surface of the WH plant cell wall. The CLSM offers visualization of the degradation of lignin that fluoresces at 568 nm. Data and images obtained from these analyses showed the efficacy of the combined application of the pretreatment method in terms of WHB degradation, which is better than individual chemical pretreatment. For the future, these findings showed the significant potential of using an integrated tool with chemical and biological pretreatment for large scale utilization and bioconversion of this



potential aquatic weed for bioenergy production. Therefore, the effectiveness of biological pretreatment for a lignocellulosic weedy biomass like WHB can be concluded and this approach could be recommended to produce bioethanol.

**Author Contributions:** Conceptualization, A.K.; Formal analysis, A.M.F.N.; Investigation, J.K.S. and B.C.; Methodology, J.K.S. and B.C.; Software, A.M.F.N.; Supervision, A.K.; Validation, A.G., R.K., C.P.U., A.H., A.A.A., and E.F.A.A.; Writing—original draft, A.D. and A.K.; Writing—review & editing, A.D., A.M.F.N., and A.K. All authors have read and agreed to the published version of the manuscript.

**Funding:** This research was funded by University Fellowship (J.K.S.) as well as UGC Startup Grant (A.K.).

**Acknowledgments:** J.S. would like to acknowledge UGC for financial support through a university fellowship. A.K. would like to acknowledge the UGC Startup grant for financial support of the experimental work. The authors also would like to extend their sincere appreciation to the Researchers Supporting Project Number (RSP-2020/134), King Saud University, Riyadh, Saudi Arabia.

**Conflicts of Interest:** The authors declare that they have no competing interests.

### Abbreviations

WHB	Water Hyacinth Biomass
FTIR	Fourier Transform Infrared Spectrometer
SEM	Scanning Electron Microscopy
CLSM	Confocal Laser Scanning Microscope
XRD	X-ray Diffraction

### References

- Singh, N.B.; Kumar, A.; Rai, S. Potential production of bioenergy from biomass in an Indian perspective. *Renew. Sustain. Energy Rev.* **2014**, *39*, 65–78. [[CrossRef](#)]
- Kumar, A.; Sharma, S. Potential non-edible oil resources as biodiesel feedstock: An Indian perspective. *Renew. Sustain. Energy Rev.* **2011**, *15*, 1791–1800. [[CrossRef](#)]
- Kumar, A.; Kumar, K.; Kaushik, N.; Sharma, S.; Mishra, S. Renewable energy in India: Current status and future potentials. *Renew. Sustain. Energy Rev.* **2010**, *14*, 2434–2442. [[CrossRef](#)]
- Ahmad, S.; Pathak, V.V.; Kothari, R.; Kumar, A.; Krishna, S.B.N. Optimization of nutrient stress using *C. pyrenoidosa* for lipid and biodiesel production in integration with remediation in dairy industry wastewater using response surface methodology. *3 Biotech* **2018**, *8*, 326. [[CrossRef](#)]
- Singh, J.K.; Vyas, P.; Dubey, A.; Upadhyaya, C.P.; Kothari, R.; Tyagi, V.V.; Kumar, A. Assessment of different pretreatment technologies for efficient bioconversion of lignocellulose to ethanol. *Front. Biosci. Sch.* **2018**, 350–371. [[CrossRef](#)]
- Vasudevan, P.; Sharma, S.; Kumar, A. Liquid fuel from biomass: An overview. *J. Sci. Ind. Res.* **2005**, *64*, 822–831.
- Tiwari, G.; Sharma, A.; Kumar, A.; Sharma, S. Assessment of microwave-assisted alkali pretreatment for the production of sugars from banana fruit peel waste. *Biofuels* **2019**, 1–8. [[CrossRef](#)]
- Singh, J.K.; Sharma, R.K.; Ghosh, P.; Kumar, A.; Khan, M.L. Imidazolium Based Ionic Liquids: A Promising Green Solvent for Water Hyacinth Biomass Deconstruction. *Front. Chem.* **2018**, *6*. [[CrossRef](#)]
- Kothari, R.; Ahmad, S.; Pathak, V.V.; Pandey, A.; Kumar, A.; Shankarayan, R.; Black, P.N.; Tyagi, V.V. Algal-based biofuel generation through flue gas and wastewater utilization: A sustainable prospective approach. *Biomass Convers. Biorefinery* **2019**, 1–24. [[CrossRef](#)]
- Awasthi, M.; Kaur, J.; Rana, S. Bioethanol Production Through Water Hyacinth, Eichhornia Crassipes Via Optimization of the Pretreatment Conditions. *Int. J. Emerg. Technol. Adv. Eng.* **2013**, *3*, 42–46.
- Bardant, T.B.; Rinaldi, N.; Sarwono, R. Optimization of water hyacinth utilization in bioethanol production by using cheminformatics approach. In Proceedings of the AIP Conference, Yogyakarta, Indonesia, 7 November 2018.
- Guragain, Y.N.; De Coninck, J.; Husson, F.; Durand, A.; Rakshit, S.K. Comparison of some new pretreatment methods for second generation bioethanol production from wheat straw and water hyacinth. *Bioresour. Technol.* **2011**, *102*, 4416–4424. [[CrossRef](#)] [[PubMed](#)]
- Ruan, T.; Zeng, R.; Yin, X.-Y.; Zhang, S.-X.; Yang, Z.-H. Water Hyacinth (*Eichhornia crassipes*) Biomass as a Biofuel Feedstock by Enzymatic Hydrolysis. *BioResources* **2016**, *11*, 2372–2380. [[CrossRef](#)]
- Gupta, A.; Sharma, S.; Kumar, A.; Alam, P.; Ahmad, P. Enhancing nutritional contents of *Lentinus sajor-caju* using residual biogas slurry waste of detoxified mahua cake mixed with wheat straw. *Front. Microbiol.* **2016**, *7*, 1529. [[CrossRef](#)] [[PubMed](#)]
- Ali, S.S.; Nessem, A.A.; Sun, J.; Li, X. The effects of water hyacinth pretreated digestate on *Lupinus termis* L. seedlings under salinity stress: A complementary study. *J. Environ. Chem. Eng.* **2019**, *7*, 103159. [[CrossRef](#)]

16. Oroka, F. Fuel Briquettes from Water Hyacinth-Cow Dung Mixture as Alternative Energy for Domestic and Agro-Industrial Applications. *J. Energy Technol. Policy* **2013**, *3*, 2224–3232.
17. Shanab, S.M.M.; Hanafy, E.A.; Shalaby, E.A. Water Hyacinth as Non-edible Source for Biofuel Production. *Waste Biomass Valorization* **2018**, *9*, 255–264. [[CrossRef](#)]
18. Tobias, V.D.; Conrad, J.L.; Mahardja, B.; Khanna, S. Impacts of water hyacinth treatment on water quality in a tidal estuarine environment. *Biol. Invasions* **2019**, *21*, 3479–3490. [[CrossRef](#)]
19. Binod, P.; Janu, K.U.; Sindhu, R.; Pandey, A. Hydrolysis of lignocellulosic biomass for bioethanol production. In *Biofuels*; Academic Press: Cambridge, MA, USA, 2011; ISBN 9780123850997.
20. Vyas, P.; Kumar, A.; Singh, S. Biomass breakdown: A review on pretreatment, instrumentations and methods. *Front. Biosci. Elit.* **2018**, *1*, 155–174. [[CrossRef](#)]
21. Sticklen, M.B. Plant genetic engineering for biofuel production: Towards affordable cellulosic ethanol. *Nat. Rev. Genet.* **2018**, *10*, 155–174. [[CrossRef](#)]
22. Biswas, B.; Kumar Banik, A.; Biswas, B. Comparative study of various pre-treatment techniques for saccharifications of water hyacinth (*Eichhornia crassipes*) cellulose. *Int. J. Biotech Trends Technol.* **2015**, *44*, 283–289.
23. Yan, J.; Wei, Z.; Wang, Q.; He, M.; Li, S.; Irbis, C. Bioethanol production from sodium hydroxide/hydrogen peroxide-pretreated water hyacinth via simultaneous saccharification and fermentation with a newly isolated thermotolerant *Kluyveromyces marxianus* strain. *Bioresour. Technol.* **2015**, *193*, 103–109. [[CrossRef](#)] [[PubMed](#)]
24. Das, A.; Ghosh, P.; Paul, T.; Ghosh, U.; Pati, B.R.; Mondal, K.C. Production of bioethanol as useful biofuel through the bioconversion of water hyacinth (*Eichhornia crassipes*). *3 Biotech* **2016**, *6*, 70. [[CrossRef](#)] [[PubMed](#)]
25. Narra, M.; Divecha, J.; Shah, D.; Balasubramanian, V.; Vyas, B.; Harijan, M.; Macwan, K. Cellulase production, simultaneous saccharification and fermentation in a single vessel: A new approach for production of bio-ethanol from mild alkali pre-treated water hyacinth. *J. Environ. Chem. Eng.* **2017**, *5*, 2176–2181. [[CrossRef](#)]
26. Mansikkamäki, P.; Lahtinen, M.; Rissanen, K. The conversion from cellulose I to cellulose II in NaOH mercerization performed in alcohol–water systems: An X-ray powder diffraction study. *Carbohydr. Polym.* **2007**, *68*, 35–43. [[CrossRef](#)]
27. Vyas, P.; Kumar, D.; Dubey, A.; Kumar, A. Screening and Characterization of *Achromobacter xylosoxidans* isolated from rhizosphere of *Jatropha curcas* L. (Energy Crop) for plant-growth-promoting traits. *J. Adv. Res. Biotechnol.* **2018**, *3*, 1–8. [[CrossRef](#)]
28. Saha, B.C.; Qureshi, N.; Kennedy, G.J.; Cotta, M.A. Biological pretreatment of corn stover with white-rot fungus for improved enzymatic hydrolysis. *Int. Biodeterior. Biodegrad.* **2016**, *109*, 29–35. [[CrossRef](#)]
29. Kasana, R.C.; Salwan, R.; Dhar, H.; Dutt, S.; Gulati, A. A rapid and easy method for the detection of microbial cellulases on agar plates using Gram's iodine. *Curr. Microbiol.* **2008**, *57*, 503–507. [[CrossRef](#)]
30. Letunic, I.; Bork, P. Interactive Tree Of Life (iTOL) v4: Recent updates and new developments. *Nucleic Acids Res.* **2019**, *47*, W256–W259. [[CrossRef](#)]
31. de Carvalho, D.M.; de Queiroz, J.H.; Colodette, J.L. Assessment of alkaline pretreatment for the production of bioethanol from eucalyptus, sugarcane bagasse and sugarcane straw. *Ind. Crop. Prod.* **2016**, *94*, 932–941. [[CrossRef](#)]
32. Phitsuwan, P.; Permsriburasak, C.; Baramee, S.; Teeravivattanakit, T.; Ratanakhanokchai, K. Structural Analysis of Alkaline Pretreated Rice Straw for Ethanol Production. *Int. J. Polym. Sci.* **2017**, *2017*, 1–9. [[CrossRef](#)]
33. Ferrer, A.; Alciaturi, C.; Faneite, A.; Rios, J. Analyses of Biomass Fibers by XRD, FT-IR, and NIR. In *Analytical Techniques and Methods for Biomass*; Vaz, S., Jr., Ed.; Springer International Publishing: Cham, Switzerland, 2016; pp. 45–83, ISBN 978-3-319-41414-0.
34. Nelson, M.L.; O'Connor, R.T. Relation of certain infrared bands to cellulose crystallinity and crystal lattice type. Part II. A new infrared ratio for estimation of crystallinity in celluloses I and II. *J. Appl. Polym. Sci.* **1964**, *8*, 1325–1341. [[CrossRef](#)]
35. Segal, L.; Creely, J.J.; Martin, A.E.; Conrad, C.M. An Empirical Method for Estimating the Degree of Crystallinity of Native Cellulose Using the X-ray Diffractometer. *Text. Res. J.* **1959**, *29*, 786–794. [[CrossRef](#)]
36. Landis, C.A. Graphitization of dispersed carbonaceous material in metamorphic rocks. *Contrib. Mineral. Petrol.* **1971**, *30*, 34–45. [[CrossRef](#)]
37. Chum, H.L.; Johnson, D.K.; Black, S.K.; Overend, R.P. Pretreatment-Catalyst effects and the combined severity parameter. *Appl. Biochem. Biotechnol.* **1990**, 1–14. [[CrossRef](#)]
38. Orozco, R.S.; Hernández, P.B.; Morales, G.R.; Núñez, F.U.; Villafuerte, J.O.; Lugo, V.L.; Ramírez, N.F.; Díaz, C.E.B.; Vázquez, P.C. Characterization of lignocellulosic fruit waste as an alternative feedstock for bioethanol production. *BioResources* **2014**, *9*, 1873–1885. [[CrossRef](#)]
39. Åkerholm, M.; Hinterstoisser, B.; Salmén, L. Characterization of the crystalline structure of cellulose using static and dynamic FT-IR spectroscopy. *Carbohydr. Res.* **2004**, *339*, 569–578. [[CrossRef](#)]
40. Hurtubise, F.G.; Krassig, H. Classification of Fine Structural Characteristics in Cellulose by Infrared Spectroscopy. Use of Potassium Bromide Pellet Technique. *Anal. Chem.* **1960**, *32*, 177–181. [[CrossRef](#)]
41. Nada, A.M.A.; Mohamed, S.H.; Abd El Mongy, S.; Seoudi, R. Preparation, vibrational structure and dielectric properties studies of cotton linter and its derivatives. *J. Non. Cryst. Solids* **2009**, *355*, 2544–2549. [[CrossRef](#)]
42. Oh, S.Y.; Yoo, D.I.; Shin, Y.; Seo, G. FTIR analysis of cellulose treated with sodium hydroxide and carbon dioxide. *Carbohydr. Res.* **2005**, *340*, 417–428. [[CrossRef](#)]
43. Carrillo, F.; Colom, X.; Suñol, J.J.; Saurina, J. Structural FTIR analysis and thermal characterisation of lyocell and viscose-type fibres. *Eur. Polym. J.* **2004**, *40*, 2229–2234. [[CrossRef](#)]

44. Zhang, Y.H.P.; Ding, S.Y.; Mielenz, J.R.; Cui, J.B.; Elander, R.T.; Laser, M.; Himmel, M.E.; McMillan, J.R.; Lynd, L.R. Fractionating recalcitrant lignocellulose at modest reaction conditions. *Biotechnol. Bioeng.* **2007**, *97*, 214–223. [[CrossRef](#)] [[PubMed](#)]
45. Pothiraj, C.; Arumugam, R.; Gobinath, M. Sustaining ethanol production from lime pretreated water hyacinth biomass using mono and co-cultures of isolated fungal strains with *Pichia stipitis*. *Bioresour. Bioprocess.* **2014**, *1*, 27. [[CrossRef](#)]
46. Manivannan, A.; Narendhirakannan, R.T. Bioethanol Production from Aquatic Weed Water Hyacinth (*Eichhornia crassipes*) by Yeast Fermentation. *Waste Biomass Valorization* **2015**, *6*, 209–216. [[CrossRef](#)]
47. Marchessault, R.H.; Sarko, A. X-ray Structure of Polysaccharides. In *Advances in Carbohydrate Chemistry*; Wolfson, M.L., Tipson, R.S., Eds.; Academic Press: Cambridge, MA, USA, 1967; Volume 22, pp. 421–482.
48. Langan, P.; Nishiyama, Y.; Chanzy, H. X-ray Structure of Mercerized Cellulose II at 1 Å Resolution. *Biomacromolecules* **2001**, *2*, 410–416. [[CrossRef](#)]
49. Sindhu, R.; Binod, P.; Pandey, A. Biological pretreatment of lignocellulosic biomass—An overview. *Bioresour. Technol.* **2016**, *199*, 76–82. [[CrossRef](#)]
50. Maurya, D.P.; Singla, A.; Negi, S. An overview of key pretreatment processes for biological conversion of lignocellulosic biomass to bioethanol. *3 Biotech* **2015**, *5*, 597–609. [[CrossRef](#)]
51. Karimi, K.; Taherzadeh, M.J. A critical review of analytical methods in pretreatment of lignocelluloses: Composition, imaging, and crystallinity. *Bioresour. Technol.* **2016**, *200*, 1008–1018. [[CrossRef](#)]
52. Tian, Z.; Chen, J.; Ji, X.; Wang, Q.; Yang, G.; Fatehi, P. Dilute Sulfuric Acid Hydrolysis of Pennisetum (sp.). *Bioresour.* **2017**, *12*, 2609–2617. [[CrossRef](#)]
53. Baramee, S.; Siriatcharanon, A.K.; Ketbot, P.; Teeravivattanakit, T.; Waeonukul, R.; Pason, P.; Tachaapaikoon, C.; Ratanakhanokchai, K.; Phitsuwan, P. Biological pretreatment of rice straw with cellulase-free xylanolytic enzyme-producing *Bacillus firmus* K-1: Structural modification and biomass digestibility. *Renew. Energy* **2020**, *160*, 555–563. [[CrossRef](#)]
54. Taniguchi, M.; Suzuki, H.; Watanabe, D.; Sakai, K.; Hoshino, K.; Tanaka, T. Evaluation of pretreatment with *Pleurotus ostreatus* for enzymatic hydrolysis of rice straw. *J. Biosci. Bioeng.* **2005**, *100*, 637–643. [[CrossRef](#)]
55. Singh, S.; Cheng, G.; Sathitsuksanoh, N.; Wu, D.; Varanasi, P.; George, A.; Balan, V.; Gao, X.; Kumar, R.; Dale, B.E.; et al. Comparison of Different Biomass Pretreatment Techniques and Their Impact on Chemistry and Structure. *Front. Energy Res.* **2015**, *2*, 1–12. [[CrossRef](#)]
56. Singh, S.; Simmons, B.A.; Vogel, K.P. Visualization of biomass solubilization and cellulose regeneration during ionic liquid pretreatment of switchgrass. *Biotechnol. Bioeng.* **2009**, *104*, 68–75. [[CrossRef](#)] [[PubMed](#)]
57. Dong, M.; Wang, S.; Xu, F.; Wang, J.; Yang, N.; Li, Q.; Chen, J.; Li, W. Pretreatment of sweet sorghum straw and its enzymatic digestion: Insight into the structural changes and visualization of hydrolysis process. *Biotechnol. Biofuels* **2019**, *12*, 1–11. [[CrossRef](#)] [[PubMed](#)]